

Longitudinal momentum distributions of $^{16,18}\text{C}$ fragments after one-neutron removal from $^{17,19}\text{C}$ ^{*}

T. Baumann ^a, H. Geissel ^a, H. Lenske ^b, K. Markenroth ^c,
W. Schwab ^a, M.H. Smedberg ^c, T. Aumann ^a, L. Axelsson ^c,
U. Bergmann ^d, M.J.G. Borge ^e, D. Cortina-Gil ^a, L. Fraile ^e,
M. Hellström ^{a,1}, M. Ivanov ^f, N. Iwasa ^{a,2}, R. Janik ^f,
B. Jonson ^c, G. Münzenberg ^a, F. Nickel ^a, T. Nilsson ^g,
A. Ozawa ^h, A. Richter ⁱ, K. Riisager ^d, C. Scheidenberger ^a,
G. Schrieder ⁱ, H. Simon ⁱ, B. Sitar ^f, P. Strmen ^f, K. Sümmerer ^a,
T. Suzuki ^h, M. Winkler ^a, H. Wollnik ^j, M.V. Zhukov ^c

^a*Gesellschaft für Schwerionenforschung, D-64291 Darmstadt, Germany*

^b*Institut für Theoretische Physik I, D-35392 Giessen, Germany*

^c*Fysiska Institutionen, Chalmers Tekniska Högskola, S-41296 Göteborg, Sweden*

^d*Institut for Fysik og Astronomi, Aarhus Universitet, DK-8000 Aarhus C, Denmark*

^e*Instituto Estructura de la Materia, CSIC, E-28006 Madrid, Spain*

^f*Comenius University, 84215 Bratislava, Slovakia*

^g*EP Division, CERN, CH-1211 Genève 23, Switzerland*

^h*RIKEN, 2-1 Hirosawa, Wako, Saitama 351-01, Japan*

ⁱ*Institut für Kernphysik, Technische Universität, D-64289 Darmstadt, Germany*

^j*II. Physikalisches Institut, Universität Giessen, D-35392 Giessen, Germany*

^{*} Part of the Doctoral Thesis of T. Baumann.

¹ Present Address: Department of Physics, Lund University, S-22100 Lund, Sweden

² Present Address: RIKEN, 2-1 Hirosawa, Wako, Saitama 351-01, Japan

Abstract

The fragment separator FRS at GSI was used as an energy-loss spectrometer to measure the longitudinal momentum distributions of $^{16,18}\text{C}$ fragments after one-neutron removal reactions in $^{17,19}\text{C}$ impinging on a carbon target at about 910 MeV/u. The distributions in the projectile frames are characterized by a FWHM of 141 ± 6 MeV/ c for ^{16}C and 69 ± 3 MeV/ c for ^{18}C . The results are compared with experimental data obtained at lower energies and discussed within existing theoretical models.

PACS: 25.60.Gc, 25.70.Mn, 27.20.+n

Key words: unstable nuclei, breakup reactions, momentum distributions, nuclear structure

The dripline nucleus ^{19}C has previously been studied experimentally at MSU [1,2] and GANIL [3]. The observed momentum distributions of ^{18}C fragments and neutrons from breakup reactions were reported to be very narrow and interpreted as evidence for a one-neutron halo structure in the ^{19}C ground state. This attracted much attention because before only one case of a one-neutron halo nucleus has been confirmed experimentally, namely ^{11}Be [4]. The nucleus ^{11}Be , where relative s -motion dominates the ground state, has been subject to extensive theoretical studies over the last few years [5–9] and has provided a theoretical testing ground for one-neutron halo states.

In general, a nuclear halo state is characterized [10] by a low separation energy and low angular momentum for the valence nucleon(s). The $^{17,19}\text{C}$ isotopes have small one-neutron separation energies compared to those of the corresponding core. As an example, $S_n(^{19}\text{C}) = 242 \pm 95$ keV³ [1] which is an order of magnitude smaller than that of the core, $S_n(^{18}\text{C}) = 4180 \pm 30$ keV. Although the experimental determination of the ^{19}C mass is not very accurate, the neutron separation energy appears to be even smaller than the one for ^{11}Be ($S_n(^{11}\text{Be}) = 503 \pm 6$ keV [11]), which is a strong motivation for investigating the nuclear structure of ^{19}C .

In the present study, we have carried out measurements of the longitudinal momentum distribution of $^{16,18}\text{C}$ fragments after breakup of $^{17,19}\text{C}$. The heavy-ion synchrotron SIS at GSI delivered an ^{40}Ar primary beam at 1 GeV/u with an intensity of about $8 \cdot 10^9$ particles per spill. For the production of the secondary beam, a ^9Be target of 6.33 g/cm² thickness was placed at the entrance of the magnetic spectrometer FRS [12]. Figure 1 shows the experimental ar-

³ This value is based on the four existing mass determinations [3], while the latest NUBASE evaluation [11] gives the value $S_n(^{19}\text{C}) = 160 \pm 110$ keV, based only on the two most recent measurements.

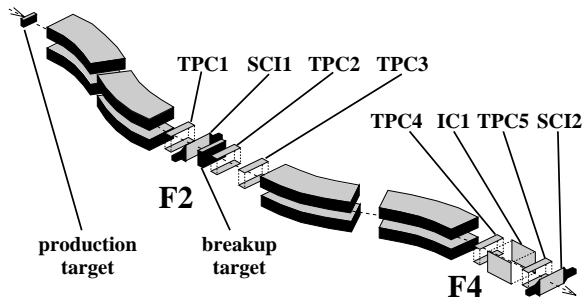


Fig. 1. Experimental setup for longitudinal momentum measurements with the FRS operated in energy-loss mode. Complete tracking of the fragments at the central focal plane (F2) and the final focus (F4) was achieved by using five time projection chambers (TPC1–TPC5). Plastic scintillators (SCI1 & SCI2) provided time-of-flight and ΔE information. Additionally, an ionization chamber (IC1) was used for the identification of the proton number.

rangement at the FRS, which was operated as an energy-loss spectrometer. In this ion-optical mode, the momentum distribution after reactions in the breakup target can be measured independently of the relatively large momentum spread of the incident secondary beam. The breakup target, 4.45 g/cm² carbon, was situated at the central focal plane (F2), where the dispersion was 7.1 m. The final focus (F4) was achromatic with respect to the production target, but had a dispersion of 5.9 m with respect to the breakup target.

For a complete tracking of the incident particles and the breakup fragments at the central focal plane, three gas-filled time projection chambers (TPC1–TPC3) were employed, one placed in front of the breakup target and two placed behind it. The TPC is a two-dimensional position sensitive detector with a homogeneous matter distribution and a resolution better than 0.5 mm in x - and y -coordinates [13]. The longitudinal momentum induced at the breakup target was determined from the positions in TPC4 and TPC5 at the final focal plane.

For the measurements of the breakup reactions, the magnetic fields of the first two dipole stages of the FRS, including quadrupole and hexapole magnets, were set to select the beams of ¹⁷C or ¹⁹C. A scintillation detector (SCI1) in front of the breakup target was used to identify the proton number Z of the incoming particles. The magnets behind the breakup target were set to a magnetic rigidity ($B\rho$) corresponding to fragments arising from a one-neutron removal of the selected projectile. Particles arriving at the final focus (F4) were identified by measuring the time-of-flight between the scintillators SCI1 and SCI2, by determining the magnetic rigidity from the position measurement, and by a coincident energy-deposition measurement in an ionisation chamber (IC1). The different isotopes were well separated in an A/Z versus Z plot. The unambiguous identification at F4, the Z -identification in front of the breakup target, and the individual $B\rho$ -settings ensured that only reaction

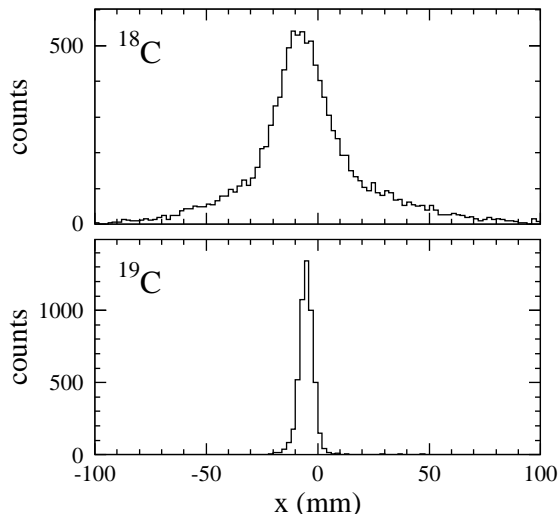


Fig. 2. Measured position distributions of $^{18,19}\text{C}$ nuclei at F4. The distribution of the ^{18}C nuclei results from the one-neutron removal reaction of ^{19}C , whereas the ^{19}C distribution corresponds to a different $B\rho$ setting of the FRS selecting the fragments which penetrated the breakup target without nuclear reactions.

products from a one-neutron removal contributed to the measured momentum distributions. The $B\rho$ -measurement was calibrated using the primary beam at different energies. The achromatism and the dispersions of the ion-optical system were experimentally deduced by transmitting the ^{17}C and the ^{19}C beam to the final focal plane (Fig. 2, bottom panel).

The momentum distribution of the core fragments is directly deduced from the position measurements with TPC4 and TPC5 using the experimentally determined dispersion at the final focus. Ion-optical aberrations, atomic energy straggling, and angular straggling in the relatively thick breakup target limit the resolution that can be achieved in this measurement. These contributions, which broaden the measured widths by about 3%, were quantified by measuring the position distributions of ^{17}C and ^{19}C nuclei that penetrated the breakup target without nuclear reactions. In Fig. 2, the measured position distribution of ^{19}C at F4 is presented together with the corresponding distribution of the ^{18}C fragments.

The breakup of the projectile nuclei is statistically distributed along their path inside the target. This causes an additional energy straggling due to the difference in energy loss between the nuclei before and after one-neutron removal. For this, we computed a negligible contribution for the momentum of $\Delta p/p = 0.5 \cdot 10^{-3}$ by applying the ion-optical ray tracing code MOCADI [14].

The longitudinal momentum distribution of ^{16}C fragments from the breakup

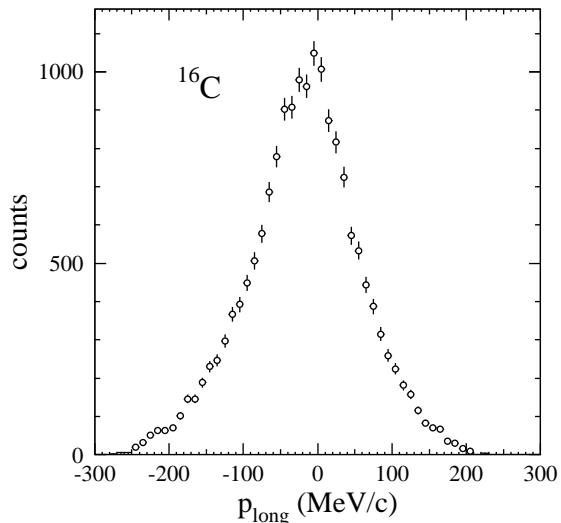


Fig. 3. Momentum spectrum of ^{16}C after one-neutron removal from ^{17}C . The FWHM, corrected for the experimental resolution, is 141 ± 6 MeV/ c .

of ^{17}C is shown in Fig. 3. This momentum distribution, which is transformed into the ^{17}C projectile frame, exhibits neither a pure Lorentzian nor a Gaussian distribution. Using a combination of two Gaussian distributions, we could reproduce the shape and determined a FWHM of 145 ± 6 MeV/ c . After correction for the experimental resolution mentioned above, this gives a FWHM of 141 ± 6 MeV/ c . This value agrees very well with a recent experiment at 84 MeV/u beam energy, where a FWHM of 145 ± 5 MeV/ c was obtained [2]. There also exists a published result from an earlier measurement of ^{17}C at low energies [1], but this value suffers from a poor identification as stated in Ref. [2] and should not be used for this comparison.

Figure 4 presents the momentum distribution of ^{18}C , transformed into the ^{19}C projectile frame. In order to cover a larger range of momenta, this distribution was recorded at two different $B\rho$ -settings for the magnetic stages behind the breakup target. The two spectra that form the combined distribution were normalized using the total particle count rate at F2.

The shape of the momentum distribution of ^{18}C fragments is well reproduced by a Lorentzian between -250 MeV/ c and $+250$ MeV/ c . The FWHM of this distribution is 71 ± 3 MeV/ c , yielding 69 ± 3 MeV/ c with the experimental resolution taken into account. This width is about 3 times smaller than the one obtained from the statistical model of Goldhaber [15] with the refined parameterization of Morrissey [16], which in general gives a good description of experimental results for tightly bound nucleons.

The measured width for the ^{19}C breakup agrees with the neutron momentum width of 64 ± 17 MeV/ c (FWHM) obtained in an experiment at 30 MeV/u [3].

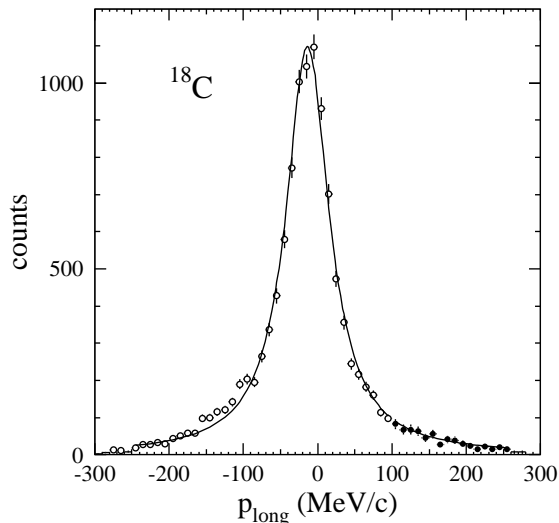


Fig. 4. Momentum spectrum of ^{18}C after one-neutron removal from ^{19}C . The distribution, transformed to the reference frame of the ^{19}C fragments, consists of a combination of two spectra recorded at two $B\rho$ settings of the fields to include also the tails of the distribution. The result of a Lorentzian fit with a FWHM of 71 ± 3 MeV/ c is shown as a solid line. With the correction for experimental resolution taken into account, the resulting FWHM is 69 ± 3 MeV/ c .

However, it is significantly larger than the result of the investigation of ^{19}C at an energy of 77 MeV/u, where a FWHM of 42 ± 4 MeV/ c (c.m. frame) was reported. This value is based on the first measurement of the nuclear breakup of ^{19}C (see Ref. [1]), but the data have been revised in a later publication [2], to which we refer here.

The main differences between Refs. [1,2] and our measurement are the projectile energies (77 MeV/u and 914 MeV/u) and the target materials (beryllium and carbon). In earlier measurements of longitudinal momentum distributions for the halo nuclei ^{11}Be and ^{11}Li , no significant dependence of the width on beam energy or target material has been observed. The effects of a limited spectrometer acceptance were taken into account for the results of Ref. [2]. In the case of our measurement, these effects are negligible due to the forward focussing at relativistic beam energies [18]. Nevertheless, this was carefully checked in our analysis using the complete particle tracking at the breakup target and at the final focal plane. From the agreement of the results for ^{17}C between Ref. [2] and our measurement, we conclude that systematic experimental effects can be ruled out as a cause of the difference observed for ^{19}C . One should keep in mind, however, that the statistics of Ref. [2] for ^{19}C are very low. A measurement at low energies with comparable statistics would be desirable in order to confirm or disprove this difference. We note for later use that the presently measured width for ^{19}C is considerably larger than the 43–50 MeV/ c [17,18] found for ^{11}Be in spite of the one-neutron separation energy

being a factor of about two lower in the case of ^{19}C .

It is not the aim of the present paper to provide a new attempt for a theoretical description of the structure of $^{17,19}\text{C}$ since there are several recent works that have dealt with this problem. Instead, we shall give a brief outline of the present status and comment on what we can conclude at this stage with respect to our experimental findings.

A common feature of $^{17,19}\text{C}$ is a loosely bound neutron moving outside a core which itself is already far off stability. The existence of low-lying 2^+ states in $^{16,18}\text{C}$ at 1.77 and 1.62 MeV [19,20], respectively, indicates that core polarization may play an important role in these nuclides. The ground state wave function of $^{17,19}\text{C}$ can then be expected to have $1s_{1/2}$ and $0d_{3/2,5/2}$ neutrons coupled to the 0^+ ground state and the 2_1^+ state as the dominating configurations. To illustrate the contributions to the experimental widths from the different components of the wave function, we show in Fig. 5 a calculation of the momentum widths after breakup of ^{19}C for pure s - and d -orbits as a function of the neutron separation energy. In this calculation, we used Hankel radial wave functions, which are the exact solutions of the Schrödinger equation outside the range of the potential, and introduced a lower cylindrical cutoff when transforming it to the corresponding momentum coordinates. This cutoff, estimated as the sum of the core and target radii [9], ensures that the one-neutron removal process takes place in the outer region of the wave function, keeping the core intact. The measured longitudinal momentum distribution of the ^{18}C fragment favors the $J^\pi = 3/2^+$ or $5/2^+$ scenario where the main part of the wave function ($\sim 65\%$) contains relative s -motion between the halo neutron and the 2_1^+ excited state of ^{18}C . The experimental data for one-neutron removal from ^{17}C can be reproduced by an almost pure d -wave neutron ($S_n = 0.73$ MeV) orbiting around the 0^+ ground state of ^{16}C . Inclusion of the first excited 2_1^+ state at 1.77 MeV of ^{16}C further improves the agreement with the experimental data.

Bazin *et al.* also used Hankel wave functions to fit their data [1,2]. They used shell model calculations to determine the parentage of the ground state to single particle wave functions. The best agreement with the experimental data for ^{17}C was found when a spin parity of $3/2^+$ from s - and d -wave neutrons coupled to the 2_1^+ state in ^{16}C was assumed. In the ^{19}C case, they used the WBT interaction predicting the spin parity of the ground state to be $5/2^+$ with the dominating configuration $^{18}\text{C}(2_1^+) \otimes 1s_{1/2}$. With these assumptions, they claimed to get a good fit to the width, while from our calculation (Fig. 5) we would expect a value closer to 60 MeV/ c .

Ridikas *et al.* [21,22] investigated $^{17,19}\text{C}$ in a neutron-plus-core coupling model with a deformed Wood-Saxon potential for the neutron-core interaction. Their analysis excluded a $J^\pi = 1/2^+$ for ^{17}C , while in the ^{19}C case, they concluded

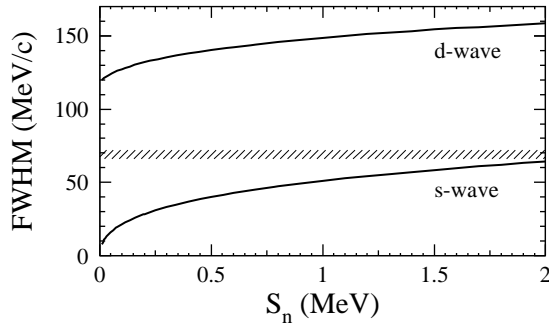


Fig. 5. Calculated momentum widths as a function of the neutron binding energy S_n for ^{18}C fragments after breakup of ^{19}C . The calculated values are for pure s - and d -orbits and the points cover the range of separation energies representing a coupling of the s - and d -state to the 0^+ ground state or the 2_1^+ state at 1.62 MeV. Note that the effective neutron separation energy of a neutron coupled to the 2_1^+ state is 1.86 MeV. Hankel wave functions with a cylindrical cutoff parameter of 5.45 fm were used in this calculation. The hatched region marks the experimental width obtained in this work.

that the main contribution to the ground state comes from relative s -motion between the halo neutron and the core, with the ^{18}C core either in its ground state or the 2_1^+ state. The calculations in Refs. [21,22] were compared to the experimental FWHM of ≈ 41 MeV/c [1], but there were difficulties to reproduce such a narrow width [22]. A better agreement with the value given in this paper is obtained if $J^\pi = 3/2^+, 5/2^+$ is assumed, and if the wave function has an appreciable amount of s -motion coupled to the 2^+ state of ^{18}C .

Describing the coupling of single particle configurations to excitations of the core nucleus by dynamical core polarization (DCP) leads to a more detailed approach. As outlined in Ref. [23] and discussed for stable nuclei in Refs. [24–27], the core–particle interactions are obtained microscopically from RPA calculations. This leads to non-static and non-local self-energies thus extending the nuclear mean-field description beyond the static Hartree-Fock approach. Dynamical core polarization is well understood for stable nuclei, where it is found to describe rather accurately single particle strength distributions of odd mass nuclei as, e. g., in Refs. [24–27].

In the DCP approach, a $1/2^+$ ground state for ^{17}C is found which, however, is almost degenerate with a nearby $5/2^+$ state at $E_x = 70$ keV. For ^{19}C , the calculations predict a $1/2^+$ ground state obtained at a separation energy $S_n = 183$ keV[28]. The first $5/2^+$ state is found about 300 keV above the ground state, and is located just beyond the continuum threshold. The $^{18}\text{C}(0^+) \otimes 1s_{1/2}$ leading particle configuration accounts for only 40% of the wave function. The $^{18}\text{C}(2_1^+) \otimes 0d_{5/2}$ core excited configuration accounts for the major part of the ^{19}C ground state. These results indicate that the binding of ^{19}C is probably

dominated by dynamical particle–core interactions rather than static mean-field dynamics. As a consequence, shell structures are dissolved and the last neutron is distributed over the single particle orbitals in the $(1s, 0d)$ -valence shell coupled to core excited configurations.

It is clear that the proximity of the s - and d -states makes it difficult to predict the ground state configurations based only on measured momentum distributions. The half-life predictions for ^{19}C are not sensitive to the ground state spin [1], and such experimental information is therefore non-conclusive. The various theoretical approaches—although being very different in detail—lead to the common conclusion that the first excited 2_1^+ state of the core plays an important role in both ^{17}C and ^{19}C . If so, the spatial extension of the halo neutron would be less than indicated by the ground state separation energy alone. The above comparison of the widths obtained for ^{19}C and ^{11}Be indeed shows that the ^{19}C ground state is a less developed one-neutron halo state.

For future experimental work, one of the challenges will be a determination of the contribution from the first excited core state, either by the observation of γ rays in coincidence with the charged fragments, or by high-resolution mass spectroscopy. Another task is to verify the experimental indication of an energy dependence of the widths, and, if this trend remains, to give a theoretical description of it.

Acknowledgements

This work was supported by the German Federal Minister for Education and Research (BMBF) under Contracts 06 DA 820, 06 OF 474, and 06 MZ 476 and by GSI via Hochschulzusammenarbeitsvereinbarungen under Contracts DARIK, OF ELK, and MZ KRK. It was partly supported by the Polish Committee of Scientific Research under Contract PB2/P03B/113/09, EC under Contract ERBCHGE-CT92-0003, CICYT under Contract AEN92-0788-C02-02 (MJGB), and by Deutsche Forschungsgemeinschaft (DFG) under Contract 436 RUS 130/127/1. One of us (B.J.) acknowledges the support through an Alexander von Humboldt Research Award.

References

- [1] D. Bazin et al., Phys. Rev. Lett. 74 (1995) 3569.
- [2] D. Bazin et al., Phys. Rev. C 57 (1998) 2156.
- [3] F.M. Marqués et al., Phys. Lett. B 381 (1996) 407.
- [4] R. Anne et al., Phys. Lett. B 304 (1993) 55.
- [5] R. Anne et al., Nucl. Phys. A 575 (1994) 125.
- [6] F.M. Nunes, I.J. Thompson and R.C. Johnson Nucl. Phys. A 596 (1995) 171.
- [7] H. Esbensen, B.A. Brown and H. Sagawa, Phys. Rev. C 51 (1995) 1274.
- [8] N.Vinh Mau, Nucl. Phys. A 592 (1995) 33.
- [9] P.G. Hansen, Phys. Rev. Lett. 77 (1996) 1016.
- [10] K. Riisager, A.S. Jensen and P. Møller, Nucl. Phys. A 548 (1992).
- [11] G. Audi et al., Nucl. Phys. A 624 (1997) 1.
- [12] H. Geissel et al., Nucl. Instr. and Meth. B 70 (1992) 286.
- [13] T. Baumann et al., Acta Physica Universitatis Comenianae XXXVII (1996) 3.
- [14] N. Iwasa et al., Nucl. Instrum. Meth. B 126 (1997) 284.
- [15] A.S. Goldhaber, Phys. Lett. B 53 (1974) 306.
- [16] D.J. Morrissey, Phys. Rev. C 39 (1989) 460.
- [17] J.H. Kelley et al., Phys. Rev. Lett. 74 (1995) 30.
- [18] H. Geissel, GSI Report 97-03 (1997) and to be published.
- [19] D.R. Tilly, H.R. Weller and C.M. Cheves, Nucl. Phys. A 564 (1993) 1.
- [20] D.R. Tilly, H.R. Weller and C.M. Cheves, Nucl. Phys. A 595 (1995) 1.
- [21] D. Ridikas et al., Europhys. Lett. 37 (1997) 385.
- [22] D. Ridikas et al., Nucl. Phys. A 628 (1998) 363.
- [23] H. Lenske, to be published in Eur. Phys. J. A.
- [24] F.J. Eckle et al., Phys. Rev. C 39 (1989) 1662.
- [25] F.J. Eckle et al., Nucl. Phys. A 506 (1990) 159.
- [26] C. Brendel et al., Nucl. Phys. A 477 (1988) 162.
- [27] P. von Neumann-Cosel et al., Nucl. Phys. A 516(1990) 385.
- [28] H. Lenske, J. Phys. G (1998), in print, and Nuovo Cimento (1998), in print.